Gridless DoA Estimation in Oversampled DFT Beamspace

Chi Wang[*†], *Zhibin Yu*[*], *Ahmed Abdelkader*[*], *Xiaofeng Wu*[*], *and Martin Haardt*[†]
[*]Munich Research Center, Huawei Technologies Duesseldorf GmbH, Munich, Germany
[†]Communications Research Laboratory, Technische Universität Ilmenau, Ilmenau, Germany
Email: {[*†]chi.wang, [†]martin.haardt}@tu-ilmenau.de
[*]{zhibinyu, ahmed.abdelkader3, xiaofeng.wu1}@huawei.com

***Abstract*—This paper extends the classical Unitary ESPRIT in DFT beamspace algorithm to the oversampled DFT beamspace. By deriving the shift-invariance property in the DFT beamspace with an arbitrary integer oversampling factor, a closed-form formulation is obtained that enables real-valued computations for high-resolution direction-of-arrival (DoA) estimation. Compared with the classical Unitary DFT ESPRIT algorithm, which is limited to an oversampling factor of 1, the proposed method projects the antenna space signals with oversampled DFT beams, allowing better focusing of the sensing power on the sector of interest (SoI). Simulations show that, when some information about the SoI is available, the proposed method significantly outperforms both antenna space ESPRIT and classical Unitary DFT ESPRIT, particularly in low SNR conditions with closely spaced sources.**

***Index Terms*—Unitary ESPRIT, oversampled DFT beamspace, gridless DoA estimation.**

I. Introduction

Accurate direction-of-arrival (DoA) estimation is beneficial for directional wireless communications, such as precise beamforming and localization. Traditional DoA estimation is often performed in the antenna element space domain, where the computational complexity increases with the number of antennas. To address this issue, beamspace processing transforms the received signals into a lower-dimensional representation, which reduces the complexity while preserving accurate estimation performance [1]. The beamforming transformation could be realized either through a digital transformation of the antenna space received signals, or via analog beamforming using analog phase shifters [2]. Since DFT beams can allow better focusing of the sensing power towards the sector of interest (SoI) [3] and can be easily implemented using analog phase shifters with discrete phases and constant amplitudes, they are commonly used for beamforming transformations. By deriving the shift-invariance property in the beamspace, closed-form gridless DoA estimation algorithms, such as beamspace ESPRIT [4] and Unitary ESPRIT [5], [6], have been developed, which allow high-resolution DoA estimation with a low computational complexity. Furthermore, oversampling in the beamspace has been introduced as an effective strategy to enhance the beamspace resolution [7]. By increasing the number of sampled beams beyond the number of physical antennas, oversampling enhances the accuracy of DoA estimation algorithms, especially in low signal-to-noise ratio (SNR) environments.

Although DFT beamspace methods have been extensively studied, the application of an oversampled DFT beamspace within the Unitary ESPRIT framework has not been addressed in prior literature. In this paper, we extend the classical Unitary ESPRIT algorithm to support DFT beamspace processing with arbitrary oversampling factors. By oversampling the DFT beamspace, the DoA estimation accuracy and the angular resolution are improved. This is due to the fact that the oversampled DFT beams focus the sensing power more efficiently on the SoI. Unlike root-MUSIC, the proposed oversampled approach enables low-complexity closed-form estimation with real-valued computations, which makes it suitable for analog beamforming systems and hardware-constrained deployments. The contributions of this paper are as follows: First, we derive the closed-form expressions for Unitary ESPRIT in the full oversampled DFT beamspace by extending the shift-invariance equations to enable arbitrary oversampling factors. Next, we provide the closed-form expressions for the reduced-dimensional selection matrices when a reduced oversampled DFT beamspace is applied to focus on a particular spatial SoI. In the following, we abbreviate classical Unitary ESPRIT in DFT beamspace, Unitary ESPRIT in oversampled DFT beamspace, and Unitary ESPRIT in antenna space (element space) as DFT-UESPRIT, DFT-O-UESPRIT, and UESPRIT, respectively.

Notation: Non-bold, lower-case bold-faced and upper-case bold-faced letters denote scalars, vectors, and matrices, respectively. The symbols $(\cdot)^H$, $(\cdot)^T$, $(\cdot)^*$ and $(\cdot)^+$ represent conjugate transpose, transpose, conjugate, and pseudo-inverse of a matrix or vector, respectively. The operator $\mathrm{diag}(\mathbf{x})$ constructs a diagonal matrix with the elements of the vector $\mathbf{x}$ on the diagonal of the matrix. For a vector $\mathbf{a}$, $[\mathbf{a}]_m$ denotes its m^{th} entry, whereas for a matrix $\mathbf{A}$, $[\mathbf{A}]_{[m,n]}$ represents its $(m,n)^{\text{th}}$ entry. The notation $\mathbf{A}(i,:)$ refers to the i-th row of a matrix $\mathbf{A}$ with all columns, and $\mathbf{A}(i,:)_{\mathbf{b}}$ refers to the i-th row of a matrix $\mathbf{A}$, with columns indexed by the numbers in the vector $\mathbf{b}$. The Matrix $\mathbf{I}_m$ denotes an identity matrix of size $m \times m$. The operators $\tan^{-1}(\cdot)$ represents inverse trigonometric functions. Furthermore, the operator $\mathbb{E}\{\cdot\}$ denotes the expectation operator, $\mathrm{Re}\{a\}$ and $\mathrm{Im}\{a\}$ denote the real and imaginary parts of a complex number a, respectively.

II. Problem Formulation

A. System Model

Consider a uniform linear array (ULA) composed of M isotropic antenna elements with an inter-element spacing of Δ. Assume that d narrowband, plane-wave signals impinge on the array with DoAs denoted by $\boldsymbol{\theta} = [\theta_1, \cdots, \theta_d]$. The received signal at time t is given by

$$\mathbf{x}(t) = \sum_{i=1}^{d} \mathbf{a}(\mu_i) s_i(t) + \mathbf{z}(t) \in \mathbb{C}^{M\times 1}, \tag{1}$$

where $s_i(t) \in \mathbb{C}$ denotes the impinging signal, and $\mathbf{a}(\mu_i) \in \mathbb{C}^{M\times 1}$ represents the array steering vector of the i-th source. For the sake of real-valued processing, we take the array center as the phase reference such that the steering vector is conjugate centrosymmetric. For instance, if the number of antennas M is odd, the steering vector is given by $\mathbf{a}(\mu_i) = \left[e^{-j(\frac{M-1}{2})\mu_i}, \cdots, e^{-j\mu_i}, 1, e^{j\mu_i}, e^{j(\frac{M-1}{2})\mu_i}\right]^T \in \mathbb{C}^{M\times 1}$, where $\mu_i = \frac{2\pi\Delta}{\lambda}\sin(\theta_i)$ denotes the spatial frequency, with λ being the wavelength, and $\mathbf{z}(t) \in \mathbb{C}^{M\times 1}$ represents zero-mean circularly symmetric complex Gaussian noise with variance σ_z^2.

By collecting N signal snapshots, the received signal in the antenna space can be expressed in matrix form as

$$\mathbf{X} = \mathbf{A}\mathbf{S} + \mathbf{Z} \in \mathbb{C}^{M\times N}, \tag{2}$$

where $\mathbf{X} = [\mathbf{x}(1), \cdots, \mathbf{x}(N)] \in \mathbb{C}^{M\times N}$ is the matrix of the received signals, $\mathbf{A} = [\mathbf{a}(\mu_1), \cdots, \mathbf{a}(\mu_d)] \in \mathbb{C}^{M\times d}$ is the steering matrix, and $\mathbf{Z} = [\mathbf{z}(1), \cdots, \mathbf{z}(N)] \in \mathbb{C}^{M\times N}$ is the noise matrix. Then, we apply the beamspace transformation to the received signals in the antenna space as follows

$$\mathbf{Y}_{\text{DFT}}^{(O)} = {\mathbf{W}_B^{(O)}}^H \mathbf{X} = {\mathbf{W}_B^{(O)}}^H \mathbf{A}\mathbf{S} + {\mathbf{W}_B^{(O)}}^H \mathbf{Z} \in \mathbb{C}^{B\times N}, \tag{3}$$

where ${\mathbf{W}_B^{(O)}}^H \in \mathbb{C}^{B\times M}$ is the DFT beamforming matrix, whose columns are a subset of the scaled DFT matrix ${\mathbf{W}_M^{(O)}}^H \in \mathbb{C}^{OM\times M}$, where B is the number of beams, and the oversampling factor is denoted by O, with $O \in \mathbb{N}$. The k-th column of $\mathbf{W}_M^{(O)}$ is given by $\mathbf{w}_k = e^{-j(\frac{M-1}{2})\gamma_k^{(O)}}[1, e^{j\gamma_k^{(O)}}, \cdots, e^{j(M-1)\gamma_k^{(O)}}]^T$ that steers at the frequency $\gamma_k^{(O)} = \frac{2\pi}{OM}k$, for $k = 0, 1, \cdots, OM-1$. Note that matrix $\mathbf{W}_M^{(O)}$ is left $\mathbf{\Pi}$-real that satisfies the condition $\mathbf{\Pi}_M \mathbf{W}_M^{(O)^*} = \mathbf{W}_M^{(O)}$, where $\mathbf{\Pi}_M \in \mathbb{R}^{M\times M}$ is the exchange matrix, with ones along its anti-diagonal and zeros elsewhere. Afterwards, we proceed to the next step of DoA estimation in DFT beamspace.

B. Review of Unitary ESPRIT in DFT Beamspace

We first review the classical DFT-UESPRIT algorithm, as the proposed method builds upon the classical one. In this context, we consider the non-oversampling case, i.e., $O = 1$. In this case, the data model (3) reduces to

$$\mathbf{Y}_{\text{DFT}}^{(1)} = {\mathbf{W}_B^{(1)}}^H \mathbf{X} = {\mathbf{W}_B^{(1)}}^H \mathbf{A}\mathbf{S} + {\mathbf{W}_B^{(1)}}^H \mathbf{Z} \in \mathbb{C}^{B\times N}. \tag{4}$$

We define $\mathbf{B}^{(1)} = {\mathbf{W}_B^{(1)}}^H \mathbf{A} \in \mathbb{R}^{B\times d}$ as the DFT beamspace steering matrix. According to [8], $\mathbf{B}^{(1)}$ satisfies a shift invariance property that can be written as

$$\mathbf{\Gamma}_1^{(1)} \mathbf{B}^{(1)} \mathbf{\Omega} = \mathbf{\Gamma}_2^{(1)} \mathbf{B}^{(1)}, \tag{5}$$

where $\mathbf{\Omega} = \text{diag}\left(\left[\tan\left(\frac{\mu_1}{2}\right), \cdots, \tan\left(\frac{\mu_d}{2}\right)\right]\right) \in \mathbb{R}^{d\times d}$, $\mathbf{\Gamma}_1^{(1)} \in \mathbb{R}^{(B-1)\times B}$ and $\mathbf{\Gamma}_2^{(1)} \in \mathbb{R}^{(B-1)\times B}$ are the pre-defined real-valued selection matrices in the reduced-dimensional DFT beamspace.

Let the d dominant left singular vectors of the real-valued matrix $[\text{Re}\{\mathbf{Y}_{\text{DFT}}^{(1)}\}, \text{Im}\{\mathbf{Y}_{\text{DFT}}^{(1)}\}]$, which automatically achieves forward-backward averaging [8], be contained in the columns of the matrix $\mathbf{U}_s^{(1)} \in \mathbb{R}^{B\times d}$. Asymptotically, $\mathbf{U}_s^{(1)}$ and $\mathbf{B}^{(1)}$ span the same d-dimensional signal subspace, implying that there exists a non-singular matrix $\mathbf{T}_B \in \mathbb{R}^{d\times d}$, such that $\mathbf{B}_M^{(1)} = \mathbf{U}_s^{(1)} \mathbf{T}_B$. Substituting this relationship into (5) yields

$$\mathbf{\Gamma}_1^{(1)} \mathbf{U}_s^{(1)} \mathbf{\Upsilon}^{(1)} = \mathbf{\Gamma}_2^{(1)} \mathbf{U}_s^{(1)}, \quad \text{where} \mathbf{\Upsilon}^{(1)} = \mathbf{T}_B \mathbf{\Omega} \mathbf{T}_B^{-1}. \tag{6}$$

Note that $\mathbf{\Omega}$ contains the eigenvalues of the solution to $\mathbf{\Upsilon}^{(1)}$, and one solution could be the Least Squares (LS) solution, given by

$$\hat{\mathbf{\Upsilon}}_{\text{LS}} = (\mathbf{\Gamma}_1^{(1)} \mathbf{U}_s^{(1)})^+ \mathbf{\Gamma}_2^{(1)} \mathbf{U}_s^{(1)}. \tag{7}$$

Then, we can estimate the spatial frequencies as follows

$$\hat{\mathbf{\Upsilon}}_{\text{LS}} = \mathbf{Q}\mathbf{\Lambda}\mathbf{Q}^{-1}, \quad \hat{\mu}_i = 2\tan^{-1}([\mathbf{\Lambda}]_{[i,i]}), \quad 1 \le i \le d, \tag{8}$$

where the first equation in (8) performs the eigenvalue decomposition (EVD).

III. Unitary ESPRIT in Oversampled DFT Beamspace

In this paper, we extend the DFT-UESPRIT algorithm to an oversampled DFT beamspace representation. The key is to extend the shift-invariance equation in (5) and derive the closed-form selection matrices when $O \ge 1$. Section III-A provides the derivation in its most general form, where the beamspace projection is based on the full oversampled DFT codebook. Section III-B discusses the reduced dimensional case, where the projection is performed by using a subset of the oversampled DFT codebook. This is typically used when the SoI is available, as it allows sufficient focusing of the sensing power over a smaller spatial coverage with oversampled DFT beams, as described in [3] for the case without oversampling.

A. Unitary ESPRIT in Full Oversampled DFT Beamspace

We define the beamspace steering vector as $\mathbf{b}_M^{(O)}(\mu_i) = {\mathbf{W}_M^{(O)}}^H \mathbf{a}(\mu_i) = [b_0^{(O)}(\mu_i), b_1^{(O)}(\mu_i), \cdots, b_{OM-1}^{(O)}(\mu_i)]^T \in \mathbb{R}^{OM\times 1}$. Then we need to find the relationship between the beamspace coefficients to derive the shift-invariance relation. When $O = 1$, the shift-invariance property relates adjacent beamspace components, namely $b_k^{(1)}(\mu_i)$ and $b_{k+1}^{(1)}(\mu_i)$. With oversampling, the adjacent components in the DFT beamspace are now separated by O indices. Therefore, to analyze the

shift-invariance relation for the oversampled case, we examine the beamspace components $b_k^{(O)}(\mu_i)$ and $b_{k+O}^{(O)}(\mu_i)$ (for $k = 0, 1, 2, \cdots, OM-1$) as follows

$$b_k^{(O)}(\mu_i) = \mathbf{w}_k^{(O)^H}\mathbf{a}(\mu_i) = \frac{\sin\left[\frac{M}{2}\left(\mu_i - k\frac{2\pi}{OM}\right)\right]}{\sin\left[\frac{1}{2}\left(\mu_i - k\frac{2\pi}{OM}\right)\right]},$$

$$\begin{aligned} b_{k+O}^{(O)}(\mu_i) = \mathbf{w}_{k+O}^{(O)^H}\mathbf{a}_M(\mu_i) &= \frac{\sin\left[\frac{M}{2}\left(\mu_i - (k+O)\frac{2\pi}{OM}\right)\right]}{\sin\left[\frac{1}{2}\left(\mu_i - (k+O)\frac{2\pi}{OM}\right)\right]} \\ &= \frac{-\sin\left[\frac{M}{2}\left(\mu_i - k\frac{2\pi}{OM}\right)\right]}{\sin\left[\frac{1}{2}\left(\mu_i - (k+O)\frac{2\pi}{OM}\right)\right]}. \end{aligned}$$

Notice that the numerator of $b_{k+O}^{(O)}(\mu_i)$ is the negative of that of $b_k^{(O)}(\mu_i)$. Therefore, these two components are related as

$$\begin{aligned} &b_k^{(O)}(\mu_i)\cdot\sin\left[\frac{1}{2}\left(\mu_i - k\cdot\frac{2\pi}{OM}\right)\right] = \\ &-b_{k+O}^{(O)}(\mu_i)\cdot\sin\left[\frac{1}{2}\left(\mu_i - (k+O)\cdot\frac{2\pi}{OM}\right)\right]. \end{aligned} \tag{9}$$

Using $\sin(\alpha-\beta) = \sin(\alpha)\cos(\beta) - \cos(\alpha)\sin(\beta)$ in (9) yields

$$\begin{aligned} &b_k^{(O)}(\mu_i)\left[\sin\left(\frac{\mu_i}{2}\right)\cos\left(\frac{\gamma_k^{(O)}}{2}\right) - \cos\left(\frac{\mu_i}{2}\right)\sin\left(\frac{\gamma_k^{(O)}}{2}\right)\right] = \\ &-b_{k+O}^{(O)}(\mu_i)\left[\sin\left(\frac{\mu_i}{2}\right)\cos\left(\frac{\gamma_{k+O}^{(O)}}{2}\right) - \cos\left(\frac{\mu_i}{2}\right)\sin\left(\frac{\gamma_{k+O}^{(O)}}{2}\right)\right], \end{aligned}$$

rearranging terms leads to

$$\begin{aligned} &\tan\left(\frac{\mu_i}{2}\right)\left[b_k^{(O)}(\mu_i)\cos\left(\frac{\gamma_k^{(O)}}{2}\right) + b_{k+O}^{(O)}(\mu_i)\cos\left(\frac{\gamma_{k+O}^{(O)}}{2}\right)\right] \\ &= b_k^{(O)}(\mu_i)\sin\left(\frac{\gamma_k^{(O)}}{2}\right) + b_{k+O}^{(O)}(\mu_i)\sin\left(\frac{\gamma_{k+O}^{(O)}}{2}\right). \end{aligned} \tag{10}$$

Hence, we could define two real-valued selection matrices $\mathbf{\Gamma}_1^{(O)}$ and $\mathbf{\Gamma}_2^{(O)}$, each of size $OM \times OM$, to relate every two components that are separated by O indices, i.e., $b_k^{(O)}(\mu_i)$ and $b_{k+O}^{(O)}(\mu_i)$. Additionally, for the components with index k starting from $(OM-O)$ to $(OM-1)$, we can compute $b_{k+O}^{(O)}(\mu_i)$ for $k = OM - O$ as

$$\begin{aligned} b_{OM}^{(O)}(\mu_i) &= \frac{\sin\left[\frac{M}{2}\left(\mu_i - OM\frac{2\pi}{OM}\right)\right]}{\sin\left[\frac{1}{2}\left(\mu_i - OM\frac{2\pi}{OM}\right)\right]} = \frac{(-1)^M\cdot\sin\left(\frac{M}{2}\mu_i\right)}{-\sin\left(\frac{1}{2}\mu_i\right)} \\ &= (-1)^{M-1}b_0^{(O)}(\mu_i), \end{aligned} \tag{11}$$

similarly, we have

$$b_{OM+1}^{(O)}(\mu_i) = (-1)^{M-1}b_1^{(O)}(\mu_i), \tag{12}$$

$$\vdots$$

$$b_{OM+O-1}^{(O)}(\mu_i) = (-1)^{M-1}b_{O-1}^{(O)}(\mu_i), \tag{13}$$

Inserting these relationships into (10) for $k \in \{OM - O, \cdots, OM-1\}$, we have equations (14) to (16) on the top of the next page. Compiling all OM equations in vector form for $0 \le k \le OM-1$ yields a shift-invariance relation for $\mathbf{b}_M^{(O)}(\mu_i)$

$$\tan\left(\frac{\mu_i}{2}\right)\mathbf{\Gamma}_1^{(O)}\mathbf{b}_M^{(O)}(\mu_i) = \mathbf{\Gamma}_2^{(O)}\mathbf{b}_M^{(O)}(\mu_i). \tag{19}$$

The selection matrices $\mathbf{\Gamma}_1^{(O)}$ and $\mathbf{\Gamma}_2^{(O)}$ for $O = 2$ are defined in equations (17) and (18) on the top of the next page, and this can be generalized to an arbitrary O by inserting $(O-1)$ zeros between two sine (or cosine) coefficients in each row of the selection matrices. Note that when $O = 1$, the selection matrices reduce to the non-oversampled case, as derived in [8]. Notice that the last O rows of $\mathbf{\Gamma}_1^{(O)}$ and $\mathbf{\Gamma}_2^{(O)}$ are a linear combination of the other rows, meaning that these selection matrices are of rank $OM - O$.

With d sources, the beamspace steering matrix is given by $\mathbf{B}_M^{(O)} = [\mathbf{b}_M^{(O)}(\mu_1), \mathbf{b}_M^{(O)}(\mu_2), \cdots, \mathbf{b}_M^{(O)}(\mu_d)] \in \mathbb{R}^{OM\times d}$. The shift-invariance relations for the steering vectors $\mathbf{b}_M^{(O)}(\mu_i)$ can be combined into a shift-invariance equation

$$\mathbf{\Gamma}_1^{(O)}\mathbf{B}_M^{(O)}\mathbf{\Omega} = \mathbf{\Gamma}_2^{(O)}\mathbf{B}_M^{(O)}, \tag{20}$$

where $\mathbf{\Omega} = \text{diag}[\left(\tan\left(\frac{\mu_1}{2}\right)\cdots\tan\left(\frac{\mu_d}{2}\right)\right)]$. Similar to Unitary DFT ESPRIT, the signal subspace $\mathbf{U}_s^{(O)}$ in the oversampled DFT beamspace is obtained as the d dominant left singular vectors of the real-valued oversampled beamspace measurement matrix $[\text{Re}\{\mathbf{Y}_{\text{DFT}}^{(O)}\}, \text{Im}\{\mathbf{Y}_{\text{DFT}}^{(O)}\}]$. Asymptotically, $\mathbf{U}_s^{(O)}$ and $\mathbf{B}_M^{(O)}$ span the same d-dimensional signal subspace, i.e., there exists a non-singular matrix $\mathbf{T}_B \in \mathbb{R}^{d\times d}$, such that $\mathbf{B}_M^{(O)} = \mathbf{U}_s^{(O)}\mathbf{T}_B$. Similar to (6), this yields

$$\mathbf{\Gamma}_1^{(O)}\mathbf{U}_s^{(O)}\mathbf{\Upsilon}^{(O)} = \mathbf{\Gamma}_2^{(O)}\mathbf{U}_s^{(O)}, \text{where}\mathbf{\Upsilon}^{(O)} = \mathbf{T}_B\mathbf{\Omega}\mathbf{T}_B^{-1}. \tag{21}$$

Following the steps (7) - (8), we can solve for $\mathbf{\Upsilon}^{(O)}$ and determine the DoAs in the oversampled DFT beamspace.

B. Unitary ESPRIT in Reduced Oversampled DFT Beamspace

Although oversampling increases the total number of beams, the reduced beamspace technique still enables dimensionality reduction. When the SoI for the DoAs is available, we can focus the sensing power on the SoI by using a selected subset of the oversampled DFT beams. This is achieved by performing the beamspace transformation using only a specific subset of the oversampled DFT codebook, and selecting only the corresponding subset of rows and columns from the selection matrices $\mathbf{\Gamma}_1^{(O)}$ and $\mathbf{\Gamma}_2^{(O)}$.

We first derive a closed-form expression for the selection matrices in the reduced beamspace. We choose B consecutive beams from the rows of the oversampled DFT matrix $\mathbf{W}_M^{(O)^H}$ to construct a SoI. Let the indices of these chosen beams be sorted in the vector $\mathbf{b}_{\text{soi}} \in \mathbb{R}^{B\times 1}$. Notably, the condition $B > O$ must be met to ensure that at least one invariance equation can be obtained. Clearly, these B consecutive beams yield $(B-O)$ invariance equations. For the p-th invariance equation ($p = 1, 2, \cdots, B-O$), we denote that it relates i_p-th and $(i_p + O)$-th beam. Based on the definition of the selection matrices, the i_p-th row of $\mathbf{\Gamma}_{1,B}^{(O)} \in \mathbb{R}^{(B-O)\times B}$ and $\mathbf{\Gamma}_{2,B}^{(O)} \in \mathbb{R}^{(B-O)\times B}$ relate the i_p-th and (i_p+O)-th beams. Therefore, the corresponding selection matrices are derived as

$$\mathbf{\Gamma}_{1,B}^{(O)}(p,:) = \mathbf{\Gamma}_1^{(O)}(i_p,:)_{\mathbf{b}_{\text{soi}}}, \quad \mathbf{\Gamma}_{2,B}^{(O)}(p,:) = \mathbf{\Gamma}_2^{(O)}(i_p,:)_{\mathbf{b}_{\text{soi}}}. \tag{22}$$

To provide concrete examples, we illustrate the process of selecting appropriate selection matrices corresponding to the

$$\tan\left(\frac{\mu_i}{2}\right)\cdot\Big[\cos\left(\frac{\gamma^{(O)}_{OM-O}}{2}\right)\cdot b^{(O)}_{OM-O}(\mu_i)+\underbrace{\cos\left(\frac{\gamma^{(O)}_{OM}}{2}\right)\cdot b^{(O)}_{OM}(\mu_i)}_{(-1)^M b^{(O)}_0(\mu_i)}\Big]=\sin\left(\frac{\gamma^{(O)}_{OM-O}}{2}\right)\cdot b^{(O)}_{OM-O}(\mu_i)+\underbrace{\sin\left(\frac{\gamma^{(O)}_{OM}}{2}\right)\cdot b^{(O)}_{OM}(\mu_i)}_{0}, \tag{14}$$

$$\tan\left(\frac{\mu_i}{2}\right)\cdot\Big[\cos\left(\frac{\gamma^{(O)}_{OM-O+1}}{2}\right)\cdot b^{(O)}_{OM-O+1}(\mu_i)+\underbrace{\cos\left(\frac{\gamma^{(O)}_{OM+1}}{2}\right)\cdot b^{(O)}_{OM+1}(\mu_i)}_{(-1)^M\cos\left(\frac{\gamma^{(O)}_1}{2}\right)b^{(O)}_1(\mu_i)}\Big]=\sin\left(\frac{\gamma^{(O)}_{OM-O+1}}{2}\right)\cdot b^{(O)}_{OM-O+1}(\mu_i)+\underbrace{\sin\left(\frac{\gamma^{(O)}_{OM+1}}{2}\right)\cdot b^{(O)}_{OM+1}(\mu_i)}_{(-1)^M\sin\left(\frac{\gamma^{(O)}_1}{2}\right)b^{(O)}_1(\mu_i)},$$

$$\vdots \tag{15}$$

$$\tan\left(\frac{\mu_i}{2}\right)\cdot\Big[\cos\left(\frac{\gamma^{(O)}_{OM-1}}{2}\right)\cdot b^{(O)}_{OM-1}(\mu_i)+\underbrace{\cos\left(\frac{\gamma^{(O)}_{OM+O-1}}{2}\right)\cdot b^{(O)}_{OM+O-1}(\mu_i)}_{(-1)^M\cos\left(\frac{\gamma^{(O)}_{O-1}}{2}\right)b^{(O)}_{O-1}(\mu_i)}\Big]=\sin\left(\frac{\gamma^{(O)}_{OM-1}}{2}\right)\cdot b^{(O)}_{OM-1}(\mu_i)+\underbrace{\sin\left(\frac{\gamma^{(O)}_{OM+O-1}}{2}\right)\cdot b^{(O)}_{OM+O-1}(\mu_i)}_{(-1)^M\sin\left(\frac{\gamma^{(O)}_{O-1}}{2}\right)b^{(O)}_{O-1}(\mu_i)},$$

(16)

$$\mathbf{\Gamma}^{(2)}_1=\begin{bmatrix}
1 & 0 & \cos\left(\frac{\gamma^{(2)}_2}{2}\right) & 0 & \cdots & 0 & 0 & 0\\
0 & \cos\left(\frac{\gamma^{(2)}_1}{2}\right) & 0 & \cos\left(\frac{\gamma^{(2)}_3}{2}\right) & \cdots & 0 & 0 & 0\\
\vdots & \vdots & \vdots & \vdots & \cdots & \vdots & \vdots & \vdots\\
0 & 0 & 0 & 0 & \cdots & \cos\left(\frac{\gamma^{(2)}_{2M-3}}{2}\right) & 0 & \cos\left(\frac{\gamma^{(2)}_{2M-1}}{2}\right)\\
(-1)^M & 0 & 0 & 0 & \cdots & 0 & \cos\left(\frac{\gamma^{(2)}_{2M-2}}{2}\right) & 0\\
0 & (-1)^M\cos\left(\frac{\gamma^{(2)}_1}{2}\right) & 0 & 0 & \cdots & 0 & 0 & \cos\left(\frac{\gamma^{(2)}_{2M-1}}{2}\right)
\end{bmatrix} \tag{17}$$

$$\mathbf{\Gamma}^{(2)}_2=\begin{bmatrix}
0 & 0 & \sin\left(\frac{\gamma^{(2)}_2}{2}\right) & 0 & \cdots & 0 & 0 & 0\\
0 & \sin\left(\frac{\gamma^{(2)}_1}{2}\right) & 0 & \sin\left(\frac{\gamma^{(2)}_3}{2}\right) & \cdots & 0 & 0 & 0\\
\vdots & \vdots & \vdots & \vdots & \cdots & \vdots & \vdots & \vdots\\
0 & 0 & 0 & 0 & \cdots & \sin\left(\frac{\gamma^{(2)}_{2M-3}}{2}\right) & 0 & \sin\left(\frac{\gamma^{(2)}_{2M-1}}{2}\right)\\
0 & 0 & 0 & 0 & \cdots & 0 & \sin\left(\frac{\gamma^{(2)}_{2M-2}}{2}\right) & 0\\
0 & (-1)^M\sin\left(\frac{\gamma^{(2)}_1}{2}\right) & 0 & 0 & \cdots & 0 & 0 & \sin\left(\frac{\gamma^{(2)}_{2M-1}}{2}\right)
\end{bmatrix} \tag{18}$$

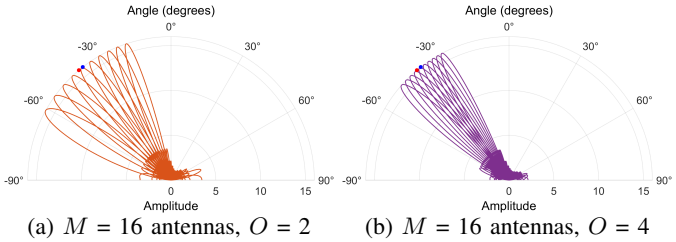

(a) M = 16 antennas, O = 2 (b) M = 16 antennas, O = 4

Fig. 1: Beam patterns of the reduced beamspace for $B = 10$ with different oversampling factors.

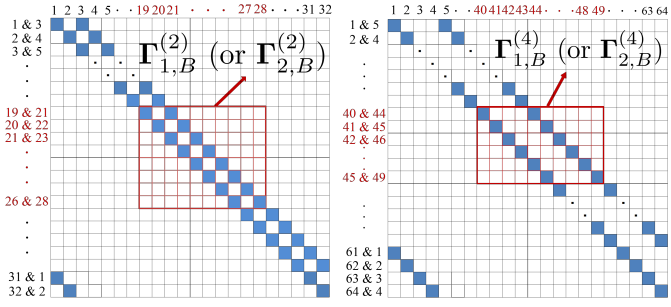

(a) M = 16 antennas, O = 2 (b) $M = 16$ antennas, $O = 4$

Fig. 2: Sparsity structure of the full-dimensional selection matrices $\mathbf{\Gamma}^{(O)}_1$ and $\mathbf{\Gamma}^{(O)}_2$ as well as examples of how to choose reduced-dimensional selection matrices of size $(B-O)\times B$ for $B = 10$.

chosen SoI. Consider a ULA with $M = 16$ antenna elements. We use two different oversampling factors, $O = 2$ and $O = 4$. For both cases, we select $B = 10$ consecutive beams to form the SoI by using specific rows from the oversampled DFT matrix. Specifically, for $O = 2$, we employ rows 19 to 28 of $\mathbf{W}^{(2)H}_M \in \mathbb{C}^{32\times 16}$, and for $O = 4$, we use rows 40 to 49 of $\mathbf{W}^{(4)H}_M \in \mathbb{C}^{64\times 16}$. The corresponding beam patterns are illustrated in Fig. 1a and Fig. 1b, respectively. The sparsity structure of the complete selection matrices for different oversampling factors, namely $\mathbf{\Gamma}^{(2)}_1$ (or $\mathbf{\Gamma}^{(2)}_2$) $\in \mathbb{R}^{32\times 32}$ and $\mathbf{\Gamma}^{(4)}_1$ (or $\mathbf{\Gamma}^{(4)}_2$) $\in \mathbb{R}^{64\times 64}$, is depicted in Fig. 2a and Fig. 2b, respectively. In these figures, blue-colored blocks denote the

entries that may be nonzero, the red-colored areas represent the subblocks corresponding to the chosen SoI as shown in Fig. 1. From these subblocks, we obtain the selection matrices corresponding to the SoI. In particular, for $O = 2$, we have $\mathbf{\Gamma}_{1,B}^{(2)}$ (or $\mathbf{\Gamma}_{2,B}^{(2)}$) $\in \mathbb{R}^{8\times 10}$, and for $O = 4$, the respective selection matrices are $\mathbf{\Gamma}_{1,B}^{(4)}$ (or $\mathbf{\Gamma}_{2,B}^{(4)}$) $\in \mathbb{R}^{6\times 10}$.

IV. Simulation Results

In this section, we assess the performance of the proposed 1-D oversampled DFT ESPRIT algorithm with a focus on the DoA estimation accuracy and resolution. Simulations were conducted using a ULA with 16 antenna elements. The antenna spacing is set to $\Delta = \frac{\lambda}{2}$, and the number of snapshots per trial is $N = 100$. The accuracy of the DoA estimates is evaluated by calculating the root mean squared error (RMSE). The RMSE is computed using $20,000$ Monte-Carlo trials.

To evaluate the estimation performance of DFT-O-UESPRIT, we conduct simulations at different SNRs ranging from 0 dB to 20 dB. Two equal-power uncorrelated sources are simulated at $\theta_1 = -40°$ and $\theta_2 = -38°$. The proposed DFT-O-UESPRIT is compared with DFT-UESPRIT and UESPRIT. The oversampling factors are set to $O = 2, 4, 8$. To ensure a fair comparison, 10 beams closest to the sources are used for all oversampling factors, as well as for DFT-UESPRIT. Note that the DoAs of the sources, the corresponding beams, and the resulting reduced-dimensional selection matrices are depicted in Fig. 1 and Fig. 2 for $O = 2$ and $O = 4$. Fig. 3a shows the RMSE (in degrees) as a function of the SNR for UESPRIT, DFT-UESPRIT, and DFT-O-UESPRIT with different oversampling factors. For comparison, the deterministic Cramér-Rao bound (CRB) [9] is also shown. It is clear that the RMSE for DFT-O-UESPRIT is lower than that of the non-oversampled case, and this is more significant in the low SNR region. As the oversampling factor increases, the RMSE decreases. Furthermore, we can observe a saturation pattern for increasing oversampling factors, such as $O = 4$ and $O = 8$.

In addition, we evaluate whether DFT-O-UESPRIT provides an improved angular resolution compared to DFT-UESPRIT and UESPRIT. The simulations are conducted with a fixed SNR of 20 dB. The source separation Δ_θ represents the angular distance between two sources varying from 0.1 to 2 degrees, with the first source located at $\theta_1 = -40°$ and the second at $\theta_2 = \theta_1 + \Delta_\theta$. The results are shown in Fig. 3b. It is observed that DFT-O-UESPRIT achieves a lower RMSE than UESPRIT and DFT-UESPRIT, indicating that oversampling improves ESPRIT's resolution for closely spaced sources. Furthermore, we can also observe a performance saturation for $O = 4$ and $O = 8$.

V. Conclusions and Future Work

This paper extends the classical Unitary ESPRIT in DFT beamspace algorithm to support oversampled DFT beamspace processing with an arbitrary integer oversampling factor. By exploiting the beamspace shift-invariance property in the oversampled DFT beamspace, a closed-form formulation with real-valued selection matrices has been derived to allow gridless high-resolution DoA estimation. The derivation is not straightforward since the sparsity structure of the resulting selection matrices depends on the oversampling factor as illustrated in Fig. 2. Simulations show that, when the SoI is available or can be estimated, the proposed method significantly outperforms both UESPRIT and DFT-UESPRIT, especially in the low SNR regime with closely spaced sources.

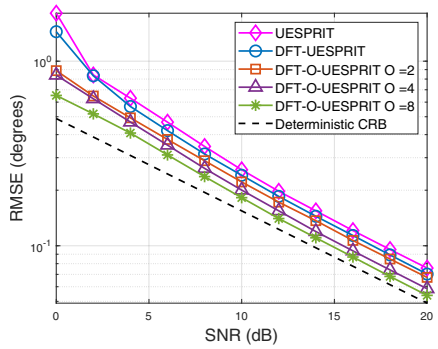

(a) RMSE vs. SNR

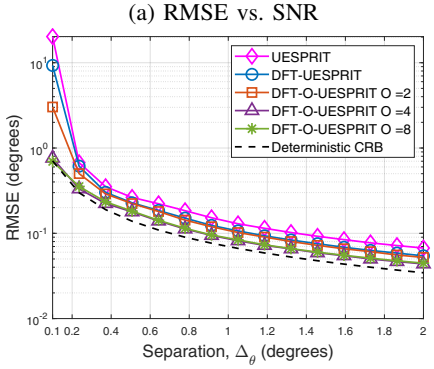

(b) RMSE vs. source separation

Fig. 3: DoA estimation accuracy comparison.

References

[1] H. L. Van Trees, "Optimum array processing," *Wiley New York*, 2002.

[2] A. Alkhateeb, O. El Ayach, G. Leus and R. W. Heath, "Channel Estimation and Hybrid Precoding for Millimeter Wave Cellular Systems," *IEEE Journal of Selected Topics in Signal Processing*, vol. 8, no. 5, pp. 831-846, Oct. 2014.

[3] J. Zhang, D. Rakhimov and M. Haardt, "Gridless Channel Estimation for Hybrid mmWave MIMO Systems via Tensor-ESPRIT Algorithms in DFT Beamspace," *IEEE Journal of Selected Topics in Signal Processing*, vol. 15, no. 3, pp. 816-831, April. 2021.

[4] Guanghan Xu, S. D. Silverstein, R. H. Roy and T. Kailath, "Beamspace ESPRIT," *IEEE Transactions on Signal Processing*, vol. 42, no. 2, pp. 349-356, Feb. 1994.

[5] M. Haardt and J. A. Nossek, "Unitary ESPRIT: how to obtain increased estimation accuracy with a reduced computational burden," *IEEE Transactions on Signal Processing*, vol. 43, no. 5, pp. 1232-1242, May 1995.

[6] J. Zhang and M. Haardt, "Channel estimation for hybrid multi-carrier mmwave MIMO systems using three-dimensional unitary esprit in DFT beamspace," in *Proc. IEEE 7th International Workshop on Computational Advances in Multi-Sensor Adaptive Processing (CAMSAP)*, Curacao, 2017, pp. 1-5.

[7] W. Ma and C. Qi, "Over-sampled beamspace channel estimation for millimeter wave massive MIMO," *IEEE International Conference on Communications (ICC)*, Kansas City, MO, USA, 2018, pp. 1-6.

[8] M. D. Zoltowski, M. Haardt, and C. P. Mathews, "Closed-form 2-D angle estimation with rectangular arrays in element space or beamspace via unitary ESPRIT," *IEEE Transactions on Signal Processing*, vol. 44, no. 2, pp. 316-328, Feb. 1996.

[9] P. Stoica and A. Nehorai, "MUSIC, maximum likelihood, Cramér-Rao bound," *IEEE Trans. Acoust., Speech, Signal Process.*, vol. 37, no. 5, pp. 720–741, May 1989.